Identification of a Dynamic Atmosphere at Enceladus with the Cassini Magnetometer

M. K. Dougherty, *et al.*

Science **311**, 1406 (2006);
DOI: 10.1126/science.1120985

REPORT

Identification of a Dynamic Atmosphere at Enceladus with the Cassini Magnetometer

M. K. Dougherty,[1*] K. K. Khurana,[2] F. M. Neubauer,[3] C. T. Russell,[2] J. Saur,[3] J. S. Leisner,[2] M. E. Burton[4]

The Cassini magnetometer has detected the interaction of the magnetospheric plasma of Saturn with an atmospheric plume at the icy moon Enceladus. This unanticipated finding, made on a distant flyby, was subsequently confirmed during two follow-on flybys, one very close to Enceladus. The magnetometer data are consistent with local outgassing activity via a plume from the surface of the moon near its south pole, as confirmed by other Cassini instruments.

Interest has been high in Cassini's observation of Saturn's moon Enceladus because of its possible contribution to the material in the E ring. The first data were obtained during a flyby on 17 February 2005 (day 48) with a closest approach altitude of 1265 km. Magnetometer observations (*1*) from this flyby revealed clear perturbations of the magnetic field, indicating that the nearly corotating plasma flow from Saturn with its frozen-in magnetic field was slowing down near Enceladus and being deflected around it. In addition, enhanced ion cyclotron wave activity at the water group gyrofrequency during the flyby indicated that Enceladus is a major source of ions for the magnetospheric plasma. A second flyby on 9 March 2005 (day 68) at an altitude of 500 km confirmed both the draping and ion cyclotron wave signatures, although clear differences between the two passes were observed. This discovery of substantial atmospheric/ion pickup acting as an obstacle to the flow of magnetospheric plasma around Enceladus led to a decision to decrease the altitude of the third Cassini flyby on 14 July 2005 (day 195) to 173 km, enabling a more detailed study of this exotic interaction by numerous onboard instruments (*2*–*6*). We describe the observations from these three flybys and offer an interpretation below.

The three Cassini flybys of Enceladus had distinct and complementary trajectories (Fig. 1). Data are shown according to the Enceladus Interaction Coordinate System (ENIS) aligned with the expected direction of the corotational flow (*7*). The first flyby was above Enceladus at about 4.7 Enceladus radii (R_E) on average above the orbital plane (*8*). The second flyby was below the moon at about 1.5 R_E, and the third flyby made a south-to-north cut as the spacecraft flew by at closest approach of about 0.7 R_E. On the last two flybys, Cassini moved inbound toward Saturn from upstream of Enceladus (as measured relative to the corotational flow), whereas on the first flyby it moved outbound. All passes moved in the direction of corotation (i.e., with increasing X in the ENIS system).

The magnetic field of Saturn at Enceladus is 325 nT due southward at the orbit of Enceladus. The perturbations that were observed during the three flybys are slight tilts of the field and a small compression of the southward field. It is most convenient for discussion to display only the perturbed field in the three directions (Fig. 1): B_X in the direction of the rotating planet, B_Y toward Saturn, and B_Z northward. The magnetic field perturbation on the first pass, day 48 of 2005, extends over a broad region from about 5 R_E inside Enceladus' orbit to about 8 R_E outside. The negative X component of the perturbed magnetic field is consistent with a slowdown of the flow below the spacecraft. The positive Y deflection of the field direction on the Saturn side and its negative Y deflection on the anti-Saturn side indicate that there is some deflection to the flow on either side of Enceladus. This signature indicates that the magnetospheric plasma that corotated with Saturn was slowed and deflected by an obstacle to the flow. Such an obstacle could be provided by an atmosphere in which ionization leads to mass loading of the magnetized plasma near Enceladus. At Enceladus one does not expect induction processes to be important because the background magnetic field has at most small deviations from axial symmetry. For a permanent dipole, a surface field on the order of ~1000 nT—as a result of remanent magnetization or a dynamo field—would be necessary to explain the first flyby observations. Neither scenario is plausible when taking into account the small size of Enceladus and its assumed internal structure and chemistry. Indeed, the second flyby observations were clearly inconsistent with the existence of a permanent dipole.

Hence, if we assume that an atmospheric interaction is occurring that caused the first flyby observations, then we may expect a scenario (Fig. 2) where Alfvén wings (*9*, *10*) above and below the conducting obstacle are generated via cur-

[1]Blackett Laboratory, Imperial College London, London SW7 2AZ, UK. [2]Institute of Geophysics and Planetary Physics, University of California, Los Angeles, CA 90025, USA. [3]Institute for Geophysics and Meteorology, Köln University, 50923 Köln, Germany. [4]Jet Propulsion Laboratory, California Institute of Technology, Pasadena, CA 91109, USA.

*To whom correspondence should be addressed. E-mail: m.dougherty@imperial.ac.uk

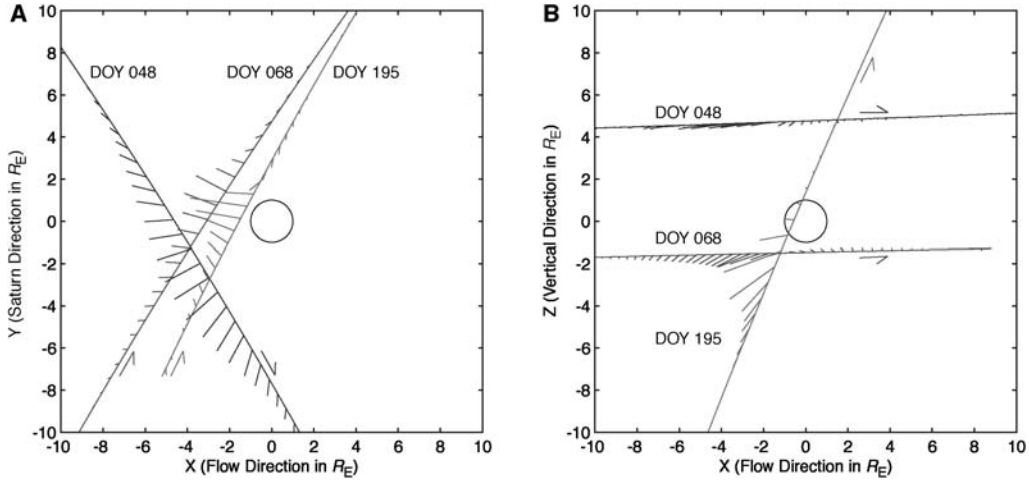

Fig. 1. (**A**) The three flyby trajectories in the (*X*, *Y*) plane of the ENIS coordinate system, where *X* is along the direction of corotational flow and *Y* is positive toward Saturn; arrows denote the flyby direction. Overlain on the trajectories are the residuals of the magnetic field (after the background magnetic field has been removed from the data). The residuals are scaled such that 4.5 nT = 2 R_E. (**B**) The three flyby trajectories in the (*X*, *Z*) plane of the ENIS coordinate system, where *X* is along the direction of corotational flow and *Z* is along Saturn's spin axis; arrows denote the flyby direction. Data are displayed as in (A).

rents that are driven through the atmosphere by the motional electric field of the incident plasma combined with the electric conductivity of the atmosphere (which in turn results from elastic collisions or ion pickup). The pickup process is connected with mass loading and has a decelerating effect on the plasma. Initial modeling suggests that the current flowing in the pickup region is on the order of 10^5 A. Pickup is also the mechanism that excites ion cyclotron waves. The electromagnetic coupling interaction between Jupiter and its volcanic moon Io is a well-known example of this type of interaction between a large moving conductor and a magnetized plasma (*11*, *12*), although at Io the currents linking the moon to Jupiter are up to 10 times as large. Ion mass loading decelerates the plasma as slow-moving, Enceladus-derived plasma is added to the faster moving magnetospheric plasma. Because the slowing is greatest where the mass loading is greatest, we would a priori expect the greatest slowing in Enceladus' orbital plane. Because the upstream field is directed southward, the B_X or along-flow component of the draped field will be negative in any plane above the mass-loading region and positive in any plane below that region (Fig. 2). In addition, above and upstream of the mass-loading region, draping will produce a positive B_Y component on the Saturnward side and a negative perturbation on the side facing away from Saturn upstream of Enceladus as the flow is decelerated to the sides of Enceladus. Finally, the field would be compressed in front of the obstacle where the magnetized plasma flow has slowed. This compression would appear mainly in the B_Z component. On the first flyby, with the Cassini spacecraft above Enceladus, we see a negative B_X, as expected, with the change in the B_Y perturbation (from negative on the negative Y side and positive on the positive Y side) indicating that the flow is being slowed and diverted around Enceladus. Moreover, the field is compressed, as expected from an upstream flyby.

The far-field signature of the Alfvén wing current system that was observed by Cassini (without actual penetration of the current-carrying wing) cannot provide detailed information about the size of the wing or the atmospheric source. Even for a strong atmospheric interaction, the necessary diameter of the atmospheric volume producing the perturbations is by necessity larger than the body of the satellite and needs to be at least on the order of ~4 R_E. A recent plasma model (*13*) predicts an even larger volume. This work suggests that a sputtering-produced atmosphere at Enceladus would not be sufficient to produce the observed magnetic field perturbations, and hence an additional atmospheric source must have been operating. A region of about 8 R_E is affected in front of and to the side of the moon, consistent with a large but weak interaction region. The magnetic field perturbations are also consistent with the conductor/atmospheric volume being south of the spacecraft trajectory and downstream of it.

The second and third flyby data sets are not as easily explained by the simple guidelines used above. The second pass on day 68 is below Enceladus (Fig. 1), and the region of strongly perturbed field is noticeably smaller and occurs inside of ~3.5 R_E. If the interaction was symmetric around Enceladus, so that the source of the slowdown was above the spacecraft,

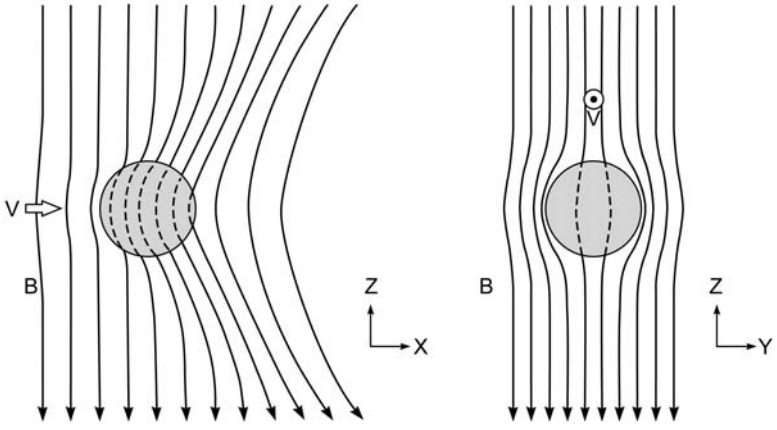

Fig. 2. A schematic showing the expected draping behavior of magnetic field lines, denoted by *B* in the vicinity of a large conducting obstacle. The left and right panels show the (*X*, *Z*) and (*Y*, *Z*) planes of the ENIS coordinate system, respectively. The inflowing corotating Saturn plasma (with velocity *V*) is slowed down with the field being draped around the obstacle. Field lines are dashed where they are moving through the conducting body.

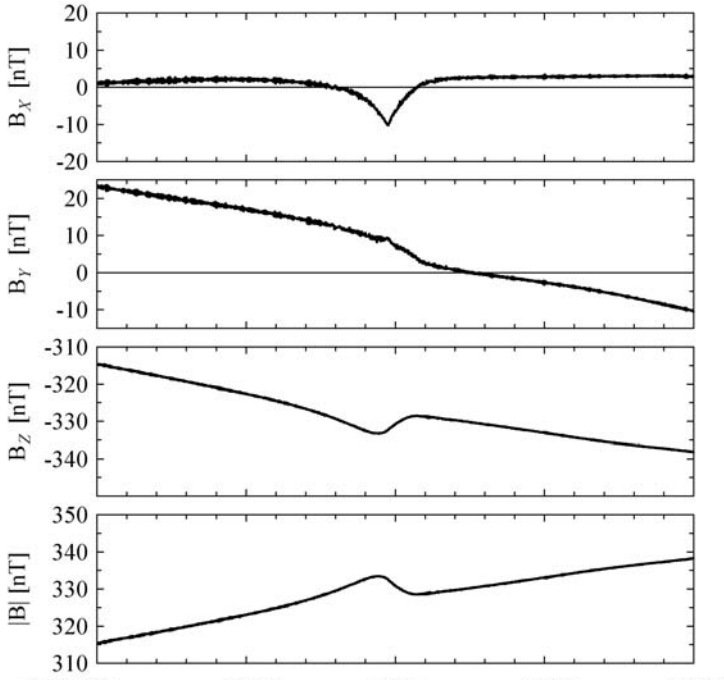

X [R_E]	-6.90	-4.10	-1.11	2.06	5.41
Y [R_E]	-10.96	-5.00	0.85	6.61	12.27
Z [R_E]	-15.90	-8.56	-1.21	6.14	13.48
R [R_E]	20.50	10.73	1.85	9.25	19.02

Fig. 3. Magnetic field data from the close flyby on day 195 in the ENIS coordinate system. The three components of the magnetic field and the absolute value of the field magnitude are shown. The clear perturbation in the magnetic field due to the interaction with Enceladus is clearly visible. Details of the spacecraft trajectory are listed beneath the plot; *R* is the radial distance of the Cassini spacecraft away from Enceladus.

then the perturbation vectors should be reversed relative to those of day 48. Outbound from about $Y = 3\ R_E$, this is true. However, inbound before $Y = 0\ R_E$, this is only partially true; B_Y appears to be in the direction for deflection around Enceladus above Cassini, but the B_X component is in the direction of slowdown below Cassini. Thus, the second flyby reveals a more complex picture. Because the major perturbation in the field appears to be in the negative B_X direction, the source is south of the spacecraft, even though the spacecraft itself is south of Enceladus. This implies the existence of a perhaps narrower pickup region extending southward, possibly due to an outgassing polar plume.

The implications of these findings, linked with the clear evidence from Voyager observations of endogenic geological activity (*14*) and speculations of outgassing or geyser-type activity, led to the decision to substantially decrease the altitude of the next Enceladus flyby. This took place on day 195 at 173 km. In the ENIS coordinate system, with the largest perturbation occurring in the B_X component, a sharp corner is seen in the minimum before closest approach (Fig. 3). These sharp gradients in the field suggest that the spacecraft may have crossed a current boundary during this time, perhaps even an entry into the atmospheric plume/ionosphere. The data on this encounter need to be visualized in three dimensions because the trajectory moves very rapidly in Z during the encounter. It can clearly be seen (Fig. 1) that the perturbation vectors are almost identical to those of day 68 despite the rapid motion in Z. The B_X perturbation is that of a slowdown in the flow below the spacecraft (while Cassini is in turn well below the orbital plane of Enceladus). Hence, the outgassing source must by necessity be at high southern latitudes well below the orbital plane. This is consistent with the realization that a neutral atmosphere at Enceladus is not strongly gravitationally bound for normal temperatures and will be even weaker for the high temperatures detected by observations (*2*, *3*) in the tiger stripes (*4*) near the south pole. However, this is not the complete story, because the B_Y perturbation is that of a deflection in Y around Enceladus but above Cassini. In other words, the perturbation in B_Y is 90° from what one would expect for a simple draping-type signature.

Ion cyclotron waves oscillating near the gyrofrequencies of water-group ions have been observed on nearly every Cassini orbit between 3.5 and 7 R_S (*15*). During the three close encounters of Enceladus, however, the waves changed in character as the spacecraft approached the moon. Near the orbit of Enceladus, the water-group waves nominally have amplitudes of ~0.25 nT. On each of the three flyby days, the wave amplitude began to increase above the background some 35 R_E away. On the first flyby, the amplitude rose to 0.72 nT at closest approach and continued increasing outbound from Enceladus. On the second flyby, the amplitude at closest approach was 0.34 nT; on the third flyby, the amplitude increased to a maximum of 0.55 nT but decreased to 0.32 nT at closest approach.

Because wave growth increases as pickup rate and background flow speed increase, the observed decrease on day 195 may result from a decrease in either the pickup rate or the velocity of the pickup. However, because we expect the pickup rate to monotonically increase as Enceladus is approached, we believe the decrease in wave amplitude signals a slowdown in the plasma flow near the moon. The subsolar latitude on Enceladus is about 20°S, but it has been shown (*16*) that charge exchange and electron impacts, not photoionization, would be the dominant forms of ionization (by two orders of magnitude). Therefore, any variation of wave amplitudes between the different flybys is more easily attributed to variations in the moon's neutral cloud morphology, the background plasma, and the spacecraft location relative to the flow than to any photoionization effects. The energy of an Enceladus pickup ion varies as the square of the relative velocities between the plasma and the neutrals, with about half of the energy of the pickup ion being available for wave generation (*17*). Thus, by measuring the electromagnetic energy flux of the ion cyclotron waves, we can estimate the energy flow into the picked-up ions and hence the mass addition rate. For example, with the wave amplitude on the first flyby, the production rate near Enceladus can be estimated to be about 8 times the rate observed in the E ring far from the moon. This mass addition rate varies between flybys, both near and far from Enceladus.

The Cassini magnetometer data from the three recent flybys of Enceladus are consistent with the other Cassini instrument analyses of the existence of an outgassing plume near the south pole of the moon (Fig. 4). The magnetic field observations from the first flyby are most readily interpreted in terms of an atmospheric interaction in which ions are picked up and the flow is slowed down and deflected around Enceladus. In the second and third flybys, the major perturbations that are observed are compatible with a source south of the spacecraft; the narrower extent of the perturbed region is consistent with an outgassing plume close to the south pole of Enceladus, with neutrals being ejected radially away. The B_X signature is consistent in all three flybys but is more concentrated in extent in the second two flybys, as one might expect if the plume is expanding away from cracks in the surface of the moon. The B_Z perturbations simply reflect the compression in the magnetic field, with the field compressing so as to slow and deflect the flow. The B_Y perturbations in the latter two flybys are rather more difficult to interpret and will require detailed modeling work to better understand them.

The magnetic field measurements, together with the Ultraviolet Imaging Spectrograph occultation observations (*5*) from all three flybys, suggest appreciable temporal variations in the atmospheric plume on a time scale of months. The field results are consistent with the plume location obtained from other observations (*2*, *3*, *6*): The plume is emitted from the tiger stripes or cracks on the surface close to the south pole (*4*).

Initial numerical simulations based on (*13*) quantitatively confirm our qualitative conclusions. The simulations clearly indicate that the cause of the field perturbations is an atmospheric plume originating near the south pole of Enceladus. They also show that the neutral atmosphere that is generated is a dynamic one. Data from the first flyby require a spatially broadly distributed atmosphere on the scales of R_E, and because the flyby was well north of Enceladus itself, the observations were unable to place constraints on the latitudinal extent of the atmosphere. The last two flybys were much closer to Enceladus and hence could be much more constraining, indicating the source of the magnetic field perturbations to be an atmospheric plume near the south pole of Enceladus. In addition, observations made at the last two flybys are inconsistent with the broadly distributed neutral cloud and suggest the existence of a much narrower plume, confirming the dynamic nature of the atmosphere. The dynamic nature of the Enceladus neutral cloud is also consistent with the large variation of neutrals observed re-

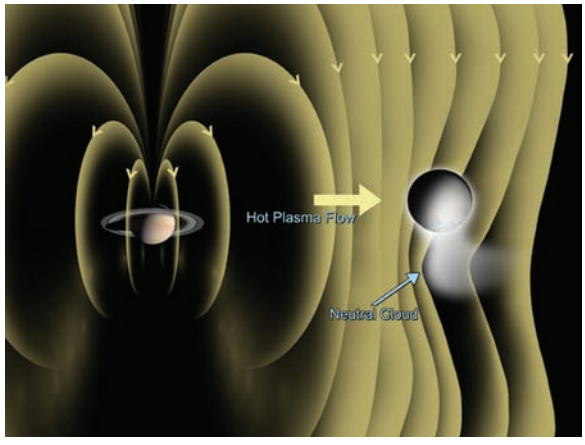

Fig. 4. A schematic (where Saturn and Enceladus are not to scale) showing the corotating Saturn magnetic field and plasma being perturbed by the neutral cloud that is produced by a polar plume generated close to the south pole of Enceladus. This scenario fits the second two flyby observations.

motely (*18*). This substantial neutral source from Enceladus may go some way toward answering one of the outstanding questions regarding our understanding of Saturn's magnetosphere: What is the missing source of the large densities of water and its derivatives that are observed?

References and Notes

1. M. K. Dougherty *et al.*, *Space Sci. Rev.* **114**, 331 (2004).
2. J. R. Spencer *et al.*, *Science* **311**, 1401 (2006).
3. R. H. Brown *et al.*, *Science* **311**, 1425 (2006).
4. C. C. Porco *et al.*, *Science* **311**, 1393 (2006).
5. C. J. Hansen *et al.*, *Science* **311**, 1422 (2006).
6. J. H. Waite Jr. *et al.*, *Science* **311**, 1419 (2006).
7. ENIS is defined with X in the direction of corotational flow; Y is positive toward Saturn and Z is along Saturn's spin axis.
8. An Enceladus radius is defined as R_E = 252.1 km.
9. S. D. Drell, H. M. Foley, M. A. Ruderman, *J. Geophys. Res.* **70**, 3131 (1965).
10. F. M. Neubauer, *J. Geophys. Res.* **85**, 1171 (1980).
11. J. W. Belcher, *Science* **238**, 170 (1987).
12. M. G. Kivelson *et al.*, *J. Geophys. Res.* **106**, 26121 (2001).
13. J. Saur, D. F. Strobel, *Astrophys. J.* **620**, L115 (2005).
14. B. A. Smith *et al.*, *Science* **215**, 504 (1982).
15. A Saturn radius is defined as R_S = 60,268 km.
16. E. C. Sittler *et al.*, *J. Geophys. Res.* **109**, A01214 (2004).
17. D. E. Huddleston, R. J. Strangeway, J. Warnecke, C. T. Russell, M. G. Kivelson, *J. Geophys. Res.* **103**, 19887 (1998).
18. L. W. Esposito *et al.*, *Science* **307**, 1251 (2005); published online 16 December 2004 (10.1126/science.1105606).

5 October 2005; accepted 11 January 2006
10.1126/science.1120985

REPORT

The Interaction of the Atmosphere of Enceladus with Saturn's Plasma

R. L. Tokar,[1]* R. E. Johnson,[2] T. W. Hill,[3] D. H. Pontius,[4] W. S. Kurth,[5] F. J. Crary,[6] D. T. Young,[6] M. F. Thomsen,[1] D. B. Reisenfeld,[7] A. J. Coates,[8] G. R. Lewis,[8] E. C. Sittler,[9] D. A. Gurnett[5]

During the 14 July 2005 encounter of Cassini with Enceladus, the Cassini Plasma Spectrometer measured strong deflections in the corotating ion flow, commencing at least 27 Enceladus radii (27 × 252.1 kilometers) from Enceladus. The Cassini Radio and Plasma Wave Science instrument inferred little plasma density increase near Enceladus. These data are consistent with ion formation via charge exchange and pickup by Saturn's magnetic field. The charge exchange occurs between neutrals in the Enceladus atmosphere and corotating ions in Saturn's inner magnetosphere. Pickup ions are observed near Enceladus, and a total mass loading rate of about 100 kilograms per second (3×10^{27} H_2O molecules per second) is inferred.

Enceladus sits in an OH cloud, or torus, around Saturn that was originally detected by the Hubble Space Telescope (*1*). This cloud extends from about 3 to 8 Saturn radii [1 R_S (Saturn's radius) = 60,268 km] with maximum concentration ($\sim 10^3$ cm^{-3}) inferred near the orbit of Enceladus (3.95 R_S). The OH cloud is produced by dissociation of H_2O, and although the peak concentration suggested that the largest source of water molecules was in the region near the orbit of Enceladus, the nature of this source was unknown. Models indicate that the source region near 4 R_S must provide ~80% of the total OH source, estimated to be $\sim 0.4 \times 10^{28}$ to 1×10^{28} H_2O molecules s^{-1} (*2*, *3*).

On 14 July 2005, the Cassini spacecraft passed within 168.2 km of Enceladus, through the cloud of neutrals and plasma (Fig. 1). The orbital speed of Enceladus is 12.6 km s^{-1}, whereas the thermal plasma corotates with Saturn at 39 km s^{-1} near Enceladus. Thus, the corotating plasma overtakes Enceladus, forming a corotational wake in the positive azimuthal direction at a speed of 26.4 km s^{-1}. Cassini passed upstream of this wake (Fig. 1B). A strong enhancement in the flux of plasma ions was detected by the Cassini Plasma Spectrometer (CAPS) (*4*) in two time intervals (Fig. 1) between t_1 = 19:41 UT and t_2 = 19:46 UT and between t_3 = 20:04 UT and t_4 = 20:26 UT.

Another Cassini instrument, the Radio and Plasma Wave Science (RPWS) instrument (*5*), measured electric field fluctuations as a function of frequency and time during the Enceladus encounter (Fig. 2). We consider first the RPWS data and then return to the CAPS data. RPWS provides an estimate of the total electron density, N_e, at Cassini from the measured frequency of the upper hybrid resonance band (Fig. 2). This frequency is a known function of both the magnetic field strength (*6*) and the total electron density. The emission observed near the upper hybrid resonance frequency is complex, with a smoothly varying narrowband emission at low frequencies and a more sporadic broadband extension to higher frequencies (Fig. 2). We assume that the narrowband relative maximum in the peak near the bottom of this complex line is the upper hybrid band and that the broadband extension to higher frequencies is a thermal plasma effect. The upper hybrid band indicates that the total electron density, shown approximately by the right-hand scale, smoothly increases from about 45 cm^{-3} at 19:30 UT to about 70 cm^{-3} at 20:04 UT. There is a short period close to Enceladus when the narrowband emission is not identifiable, likely due to dust particles hitting the spacecraft. During this time, it is not possible for RPWS to precisely determine the electron density, although there does not appear to be evidence for a substantial increase in the density (>~20%) at closest approach.

The study uses electron spectrometer, ELS, and ion mass spectrometer, IMS, data from CAPS

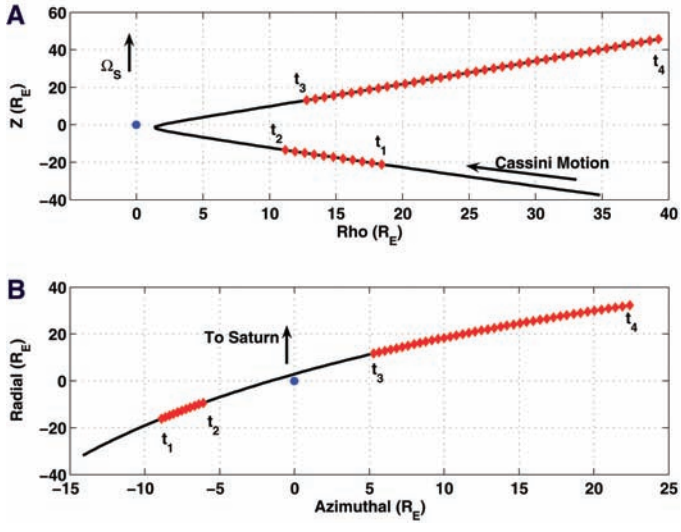

Fig. 1. Periods of CAPS-measured enhanced ion flux along the Cassini spacecraft trajectory during the close encounter of Enceladus on 14 July 2005. (**A**) An Enceladus-centered cylindrical coordinate system with the vertical axis in the direction of Saturn's spin axis and the horizontal axis the perpendicular distance from Enceladus (1 R_E = 252.1 km). (**B**) A projection into the equatorial plane with the radial coordinate positive toward Saturn and the azimuthal coordinate positive in the direction of corotation.

[1]Space Science and Applications, Los Alamos National Laboratory, Los Alamos, NM 87545, USA. [2]University of Virginia, Charlottesville, VA 22904, USA. [3]Rice University, Houston, TX 77251, USA. [4]Birmingham-Southern College, Birmingham, AL 35254, USA. [5]University of Iowa, Iowa City, IA 52242, USA. [6]Southwest Research Institute, San Antonio, TX 78228, USA. [7]University of Montana, Missoula, MT 59812, USA. [8]Mullard Space Science Laboratory, University College London, Holmbury St. Mary, Dorking, Surrey RH5 6NT, UK. [9]NASA Goddard Space Flight Center, Greenbelt, MD 20771, USA.

*To whom correspondence should be addressed. E-mail: rlt@lanl.gov